

# Relaxations in lightly crosslinked polymers

G. H. EDWARD, R. G. O'DONNELL

*Department of Materials Engineering, Monash University, Clayton, Victoria 3168, Australia*

A simple model for stress relaxation in entangled polymer melts is developed by using Gaussian statistical formulae to describe the polymer molecules, and by modelling the entanglements as energy barriers that the sliding molecules have to overcome. These entanglements are assumed to increase in number as deformation proceeds, this increase being related to loose topological knots tightening. The predictions of the model are compared with experiments conducted on plasticized poly(vinyl chloride), and with published data for a styrene-butadiene copolymer. In terms of this model, the tightening of entanglements appears to be important in polymers in which the intermolecular interactions are heterogeneous due to copolymerization or limited crystallinity, but not important in amorphous homopolymers in which entanglements are expected to be more homogeneous.

## 1. Introduction

Ferry [1] systematically analysed the mechanical behaviour of polymeric materials and classified the behaviour into a number of different regions, depending on the temperature and the time-scale of measurement. At temperatures above the glass transition all polymers exhibit a "plateau" region where the modulus is relatively independent of time or frequency, the extent of this plateau region depending significantly on the molecular weight of the polymer. The presence of a sufficient number of permanent chemical crosslinks to form a complete network broadens the plateau region.

The commonly accepted explanation for the mechanical behaviour of an uncrosslinked polymer in the plateau region is that the polymer chains undergo relaxation due to the slipping of entanglements between adjacent molecules [1, 2], these entanglements arising from topological constraints imposed on the network by interpenetration of the chain molecules.

The concept of *reptation* of an individual polymer chain [3, 4] within a tube defined by the neighbouring molecules has been introduced to model this process in a quantifiable way. The relationship between the tube model and the entanglement model has been outlined by Donth [5], who allows the cross-section of the tubes to fluctuate due to movement of the neighbouring molecules. Essentially, the most constricted portions of the tube correspond to entanglements. In this model the entanglements have two distinct modes of movement:

- (i) they can distort with the movement of the network, not altering the topology of the constraints, and
- (ii) they can slide *along* chains when two entangled chains are simultaneously in a configuration to permit slippage. The entanglement is a ring surrounding two molecules which, if momentarily parallel, will allow the ring to "slip" along the two chains. The portrayal of an entanglement as a slipping link was introduced [6] to model complicated entanglements for analysis,

where both chains were free separately to slip through the link.

In general, relaxations will occur if chain slippage occurs, although it seems to be more likely that chains will slip through entanglements in opposite directions, or that only one chain will slip rather than the entanglement slipping along two chains in the same direction as in Donth's model. A similar idea was used by Chompff and Duiser [7] who modelled an entanglement between two molecules by allowing one molecule to be completely free of the entanglement, while the other sliding molecule had a "slow point", or a viscous drag at the entanglement site.

In the following, a simple model is presented which allows relaxation due to an individual molecule slipping through an entanglement. Only the two entanglements nearest the loose end (L) are considered, one being fixed (F) and the other allowing slip (E). In many cases, a number of entanglements would be expected along a polymer chain, and the polymer chain would contract toward its centre through these entanglements if the entanglements were moved from an equilibrium separation due to some deformation process. Doi [8] gives a good account of this process for stress relaxation, but as simple considerations in the next section show, the rate of relaxation will be primarily determined by the rate of slippage of the molecule through the entanglements at the extremities of the molecule. That is, the rate of slippage of the loose or dangling ends is the important relaxation process.

The model also introduces the concept of tightening of the entanglements as deformation proceeds, by assuming that the actual number of entanglements increases with deformation. This knotting is treated here in an empirical fashion, but the predictions of this model are shown to be consistent with experiment. In general, it is expected that this process of entanglement tightening would be more important in lightly crosslinked polymer systems, where there are insuf-

ficient crosslinks to form a complete network, but the crosslinks that are present are sufficient in number to pull the entangled ends into a tight knot.

The model is treated in an elementary fashion, the main aim being to show the basic implications of the assumption of entanglement tightening. To this end, a number of simplifying assumptions are made, and so any predictions are essentially qualitative.

## 2. Theory

### 2.1. A simple model for relaxation and entanglement tightening

Consider the loose end of a chain in a polymer melt which is under no external tractions, and denote the free end of the chain by L.

At equilibrium, the chain end could be considered to have no permanent entanglements, although at any time it will in general be involved in some loose topological knots with other molecules.

On the application of a sufficiently rapid deformation the loose knots would be expected to tighten and form entanglements, in general the number and "tightness" of these knots increasing with the extent of the deformation. This would be particularly true if one part of the molecule was relatively firmly attached to surrounding molecules, as in a small crystalline region, or at a crosslink. For the moment we will assume that the knots tighten at the onset of deformation, and will allow for the deformation dependence of the tightening later.

If we assume that the entanglements form at constant contour length intervals along the molecule, the initial relaxation process can be modelled by considering the entanglement (denoted E) closest to the loose end as capable of slipping, and the next entanglement (denoted F) along the chain as fixed or permanent (see Fig. 1). This is because the relaxation of the molecule through the entanglements will be governed by the rate of slip through the endmost entanglement, where the chain section of one side of the entanglement (Section FE) will be under tension because both ends are constrained, whereas the loose end (Section EL) will (ideally) be free of tension. The molecule will relax through entanglements flanked by other entanglements much less rapidly than through the end entanglement, because the chain section on either side will be under tension. For this reason, we consider only the relaxation of the molecule through the last (end) entanglement E, adjacent to the loose end.

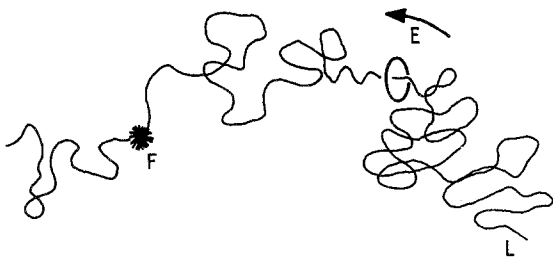


Figure 1 The fundamental unit of relaxation assumed in the model, with E being the endmost entanglement on the molecule, F the next entanglement (assumed fixed) and L the loose end of the polymer chain. Relaxation will occur by the slip of links through E from EL to FE.

If we suppose that at the stage of entanglement formation the section FE can be regarded as a Gaussian chain, then

$$|\text{FE}|^2 \equiv r_0^2 = n_0 l^2 \quad (1)$$

at the stage of the entanglements forming, where  $n_0$  is the number of random links along FE and  $l$  is the length of each link.

By introducing rectangular coordinates with origin at F, and axes parallel to the external principal strain axes, we have

$$r_0^2 = x_0^2 + y_0^2 + z_0^2 \quad (2)$$

where E has initial co-ordinates  $(x_0, y_0, z_0)$ .

Under further deformation, we assume that points E (at  $(x, y, z)$ ) and F (at the origin) move relative to each other as if embedded in an elastic continuum, that is, in an affine manner. However, during this subsequent deformation, the molecule is able to slip through E in a time-dependent way which we will picture as individual links having to surmount a potential barrier. If we define  $r$  at any stage of the deformation by

$$r^2 \equiv |\text{FE}|^2 = x^2 + y^2 + z^2 \quad (3)$$

then  $r$  can be expressed in terms of the principal extension ratios  $\lambda_1, \lambda_2$  and  $\lambda_3$  by

$$r^2 = x_0^2 \lambda_1^2 + y_0^2 \lambda_2^2 + z_0^2 \lambda_3^2 \quad (4)$$

If we now imagine our molecule to be representative of all such relaxing loose ends, and suppose that

$$x_0^2 = y_0^2 = z_0^2 = \frac{1}{3} r_0^2 = \frac{1}{3} n_0 l^2 \quad (5)$$

then Equation 4 can be simplified giving

$$r^2 = \frac{1}{3} n_0 l^2 (\lambda_1^2 + \lambda_2^2 + \lambda_3^2) \quad (6)$$

The entropy of the chain segment FE will be taken to be the Gaussian expression (for example, Treloar [9])

$$s = c - 3kr^2/2nl^2 \quad (7)$$

where  $s$  = entropy of chain,  $c$  = arbitrary constant,  $k$  = Boltzmann's constant and  $n = n(t)$  is the number of links (of length  $l$ ) in FE.

If no slipping occurs at E, then  $n = n_0$ , but here we are going to allow  $n$ , in general, to change due to relaxation of the molecule by slipping through the entanglement.

The change in entropy of such a chain from the onset of the formation of the entanglement to the current state of deformation will be given by

$$\Delta s = \frac{3k}{2l^2} \left( \frac{r^2}{n} - \frac{r_0^2}{n_0} \right) \quad (8)$$

or

$$\Delta s = -\frac{k}{2} \left[ \frac{n_0}{n} (\lambda_1^2 + \lambda_2^2 + \lambda_3^2) - 3 \right] \quad (9)$$

If there are  $N_E$  such representative entangled molecules per unit volume, then the total strain energy stored per unit volume (the strain energy function) is given by

$$W = \frac{1}{2} N_E kT \left[ \frac{n_0}{n} (\lambda_1^2 + \lambda_2^2 + \lambda_3^2) - 3 \right] \quad (10)$$

If the entanglements do not slip (and so  $n = n_0$ ), Equation 10 is identical to the familiar result obtained in the normal theory of rubber elasticity.

However, if  $n = n(t)$ , then the strain energy stored in such a slipping network will be a function of time, leading to relaxation and viscoelastic behaviour.

Equation 10 applies to the situation where  $N_E$  slipping entanglements form at the onset of deformation, with subsequent slipping occurring. However, the number of tight entanglements would be expected to increase with the amount of deformation. If we simply assume that  $N_E$  increases with the strain energy, we can write empirically

$$N_E = N_0 + N_1 \left( \frac{I - 3}{I_k - 3} \right)^q \quad \text{for } I < I_k \quad (11)$$

and

$$N_E = N_0 + N_f \quad \text{for } I \geq I_k$$

where  $N_0$  and  $N_f$  are constants,  $q$  is an empirical constant (of order unity),  $I$  is the first strain invariant defined by

$$I = \lambda_1^2 + \lambda_2^2 + \lambda_3^2 \quad (12)$$

and  $I_k$  is a critical value of  $I$  such that when  $I > I_k$  all knots have tightened.

According to Equation 11,  $N_E$  increases with the amount of deformation, and so as the later entanglements form they will undergo progressively less subsequent deformation than those formed earlier. Accordingly, Equation 10 should allow for this by dividing each extension ratio by the corresponding extension ratio at the time of entanglement tightening, and integrating over these values to find the total strain energy. The complications introduced by this are not trivial, and here it will be assumed that the form of Equation 10 is essentially correct, but that the  $n_0$  values are expected to vary somewhat to allow for the different deformations at which the entanglements tighten. This alters the single relaxation-time model outlined here to one in which a spread of relaxation times is expected.

If, in addition to a network of entanglements a material has some form of permanent crosslinking, Equation 10 could be extended to allow for this by assuming the networks (permanent and entanglement) to be in parallel, giving the strain energy function

$$W = \frac{1}{2} kT \left[ \left( N_E \frac{n_0}{n} + N_p \right) \times (\lambda_1^2 + \lambda_2^2 + \lambda_3^2) - 3 (N_E + N_p) \right] \quad (13)$$

where  $N_p$  is the number of molecular chains per unit volume in the permanent network.

In order to characterize the slip of the chain through the entanglement E, let us suppose that each link has to surmount an energy barrier in passing from one side of E to the other. To simplify the argument, allow the energy barrier to be symmetric if no net chain tension is applied at E. If no force is applied by the

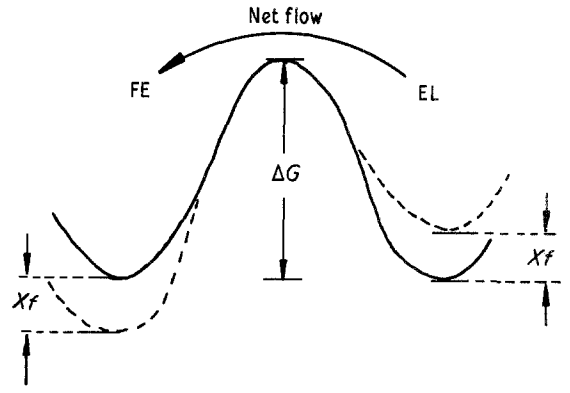


Figure 2 The symmetrical potential energy barrier to link slippage assumed to exist at E, showing the reduction in the barrier to slip from Segment EL to Segment FE caused by the tensile force  $f$  on Segment FE.

chain at E the probability of a link jumping from FE to EL would be equal to the probability of a link jumping in the opposite direction (see Fig. 2).

However, due to the constraint of both F and E being fixed (except for relative motion due to external constraints) there must be a tension along FE given by

$$f = \frac{3kTr}{nl^2} \quad (14)$$

(see, for example, Treloar [9] p. 57).

This tension will not be matched by the segment EL due to the lack of constraint on L, and so a net tension will act on the links at E, biasing the potential barrier and inducing a net flow of links into Region FE.

If the potential barrier opposing jumps from FE is increased by an amount  $Xf$ , and the potential barrier opposing jumps from EL to FE is decreased by  $Xf$ , the probability of a jump from EL to FE will be given by

$$\phi_{ELFE} = K \exp \left( - \frac{\Delta G - Xf}{kT} \right) \quad (15)$$

where  $\Delta G$  is the unperturbed potential barrier,  $K$  is a dimensionless constant and  $X$  is a constant with dimensions of length.

The probability of a jump occurring in the reverse direction will be

$$\phi_{FEEL} = K \exp \left( - \frac{\Delta G + Xf}{kT} \right) \quad (16)$$

If  $\nu$  is the frequency with which jumps occur, then the rate of change of the number of links in Region FE is given by

$$\begin{aligned} \frac{dn}{dt} &= \nu (\phi_{ELFE} - \phi_{FEEL}) \\ &= 2K\nu \exp \left( - \frac{\Delta G}{kT} \right) \sinh \left( \frac{Xf}{kT} \right) \end{aligned} \quad (17)$$

If we assume  $Xf/kT \ll 1$ , using Equations 6 and 14 this can be written as

$$\frac{n}{n_0} \frac{d}{dt} \left( \frac{n}{n_0} \right) = \frac{(\lambda_1^2 + \lambda_2^2 + \lambda_3^2)^{1/2}}{\tau} \quad (18)$$

where  $\tau$  is a temperature-dependent relaxation time given by

$$\tau = \frac{(3n_0^3)^{1/2}}{6Kv} \frac{l}{X} \exp\left(\frac{\Delta G}{kT}\right) \quad (19)$$

Equation 18 assumes that the entanglement forms at the onset of deformation, and as discussed above this is not strictly correct (see paragraph following Equation 12). Again it will be assumed that Equation 18 correctly describes the form of the change in  $n$ , but that  $n_0$  (and so  $\tau$ ) can assume a range of values. Equations 10 or 13 and 18 jointly define the way in which the strain energy relaxes for a given deformation geometry. In the following section the solution for axisymmetric stress relaxation will be obtained.

## 2.2. Axisymmetric stress relaxation

For an axisymmetric deformation along the  $x$  axis at constant volume, we have

$$\lambda_2 = \lambda_3 = \lambda_1^{-1/2} \quad (20)$$

For a stress relaxation experiment, suppose that

$$\lambda_1 = 1 \quad \text{for } t < 0$$

and

$$\lambda_1 = \lambda \quad \text{for } t \geq 0 \quad (21)$$

where  $\lambda$  is a constant.

Substitution of Equations 20 and 21 in Equation 18 gives

$$\frac{n}{n_0} \frac{d}{dt} \left( \frac{n}{n_0} \right) = \frac{1}{\tau} \left( \lambda^2 + \frac{2}{\lambda} \right)^{1/2} \quad \text{for } t \geq 0 \quad (22)$$

Integration of Equation 22 gives

$$\left( \frac{n}{n_0} \right)^2 = 1 + 2 \left( \lambda^2 + \frac{2}{\lambda} \right)^{1/2} \frac{t}{\tau} \quad (23)$$

It should be noted here that Equation 23 is valid only if  $n < 2n_0$ , because when  $n = 2n_0$  the entanglement E will have been ‘‘slipped through’’. A more detailed model should take account of this and allow for the shuffling of the links through the entanglement F. This would lead to a sequence of increasing relaxation times, and so the model is only applicable for times such that

$$t < t_c = \tau \frac{3}{2 \left( \lambda^2 + \frac{2}{\lambda} \right)^{1/2}} \quad (24)$$

Equation 24 simply ensures that  $n$  is less than  $2n_0$ . In the following this condition is not strictly adhered to, as the same qualitative predictions are valid for the larger relaxation times expected when the critical time  $t_c$  defined by Equation 24 is exceeded.

If the axisymmetric deformation is produced by one non-zero tensile force, the nominal stress  $F$  will be given by differentiation of Equation 10, giving

$$F = \left( \frac{\partial W}{\partial \lambda} \right)_{N_E, n} = N_E kT \frac{n_0}{n} \left( \lambda - \frac{1}{\lambda^2} \right) \quad (25)$$

Here we are ignoring the dependence of  $N_E$  and  $n$  on  $\lambda$ , and are calculating the force at a particular time, regarding  $N_E$  and  $n$  as constants.

Substitution of Equation 23 gives the reduced nomi-

nal stress  $f_R$  as

$$f_R \equiv \frac{F}{\lambda - \frac{1}{\lambda^2}} = N_E kT \left/ \left[ 1 + 2 \frac{t}{\tau} \left( \lambda^2 + \frac{2}{\lambda} \right)^{1/2} \right]^{1/2} \right. \quad (26)$$

In this expression,  $N_E$  is a function of  $\lambda$  which can be found by substituting Equations 20 and 21 in Equation 11, resulting in

$$N_E = N_0 + N_I \left( \frac{\lambda^2 + \frac{2}{\lambda} - 3}{\lambda_k^2 + \frac{2}{\lambda_k} - 3} \right)^q \quad \text{for } \lambda < \lambda_k$$

and

$$N_E = N_0 + N_I \quad \text{for } \lambda \geq \lambda_k \quad (27)$$

where  $\lambda_k$  is the critical value of  $\lambda$  corresponding to the critical value  $I_k$  defined by Equations 11 and 12.

The extension to a material with a permanently linked network in parallel with the entanglement network can be found by using Equation 13 instead of Equation 10, giving an extra additive term  $N_p kT$  on the right-hand side of Equation 26.

## 2.3. Predictions of model

Equations 26 and 27 taken together predict explicitly the time and extension dependence of the stress relaxation expected for a material which is undergoing relaxation due to the slipping of entanglements. Recalling Equation 19, it can be seen that the temperature dependence is also explicitly given, although that will not be pursued further here.

Firstly, if  $\lambda \geq \lambda_k$  the predicted form of the relaxation curve involves only one strain-dependent parameter, the effective relaxation time  $\tau_{\text{EFF}}$  defined by

$$\tau_{\text{EFF}} = \tau \left/ \left[ 2 \left( \lambda^2 + \frac{2}{\lambda} \right)^{1/2} \right] \right. \quad (28)$$

That is, for increasing elongation the relaxation should occur more rapidly. Secondly, if  $\lambda < \lambda_k$ , although the above strain dependence of the relaxation time still applies (Equation 28), the expression in the numerator of Equation 26 is also dependent on strain, resulting in a strain-dependent asymptote as  $t$  approaches zero on the  $\log t$  axis.

The predictions of the model are illustrated in Fig. 3, where (arbitrarily) the constants have been chosen to have the values  $N_0 kT = N_I kT = 0.5$ ;  $\lambda_k = 1.4$ ;  $\tau = 2$ ; and  $q = 1$ .

Isochronous Mooney–Rivlin plots taken from Fig. 3 are given in Fig. 4, where  $f_R$  is plotted against  $1/\lambda$  for the given values of  $t$ . Fig. 5 gives the isochronous plots obtained if  $\lambda_k$  is taken to be 1.1, all other parameters being the same as assumed before.

It can be seen that the expected isochrones have a maximum when  $\lambda = \lambda_k$ , and decrease with increasing  $\lambda$  for  $\lambda > \lambda_k$ . In the  $\lambda > \lambda_k$  region the curves are nearly linear up to quite high values of  $\lambda$ . In the following some new experimental results are reported which show a maximum in a Mooney–Rivlin plot, whereas previously reported isochrones have not demonstrated this non-monotonic behaviour.

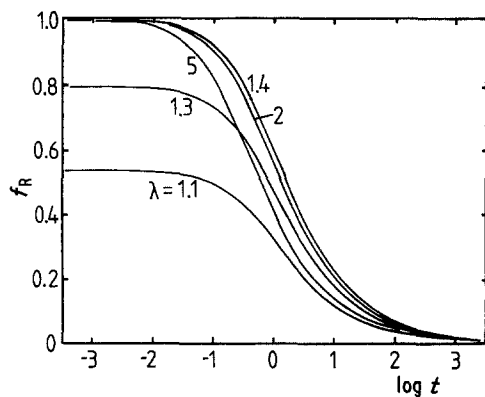


Figure 3 Stress-relaxation curves of reduced stress  $f_R$  against  $\log(t)$  predicted by the model for the indicated values of  $\lambda$ , assuming  $N_0kT = N_p kT = 0.5$ ,  $\tau = 2$ ,  $q = 1$  and  $\lambda_k = 1.4$ .

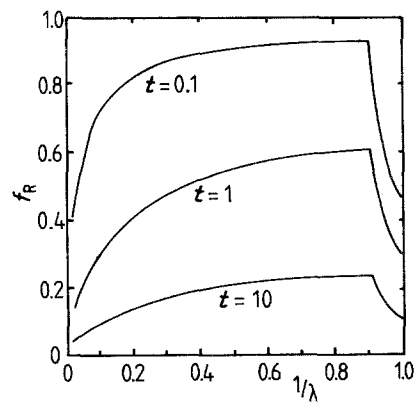


Figure 5 Isochronous Mooney-Rivlin plots for the indicated values of time, assuming  $N_0kT = N_p kT = 0.5$ ,  $\tau = 2$ ,  $q = 1$  and  $\lambda_k = 1.1$ .

### 3. Comparison with experiment

#### 3.1. Material

Simple stress-relaxation tests on plasticized poly(vinyl chloride) (PPVC) were conducted in an Instron machine at a constant room temperature of 21°C. The PVC was a commercial sheet material of about 30% plasticizer content obtained from Nyllex Australia, known as "U-V stabilized sheet". Test specimens were stamped from the sheet, giving specimens of 55 mm gauge length and 6 mm by 1 mm cross-section. Initial loading was at 50 mm min<sup>-1</sup> and the final extension was measured by using a travelling microscope to measure the distance between two marks on the gauge length of the specimen. The material was analysed using gel permeation chromatography; the number-average molecular weight was found to be  $8.09 \times 10^4$  and the weight-average molecular weight was found to be  $1.80 \times 10^5$ .

#### 3.2. Results

In Fig. 6 the results are plotted giving reduced stress as a function of  $\log(t)$  for various extensions. It can be seen that the curves "cross over" and do not display monotonic shift behaviour with increasing  $\lambda$ . This behaviour is made more clear in Fig. 7, where several isochronous curves taken from the data of Fig. 6 are given. These isochrones resemble in form those predicted by the above model, and suggest that for the plasticized PVC used here  $\lambda_k \sim 1.25$ . Using this value for  $\lambda_k$ , the predicted curves using Equations 26 and 27

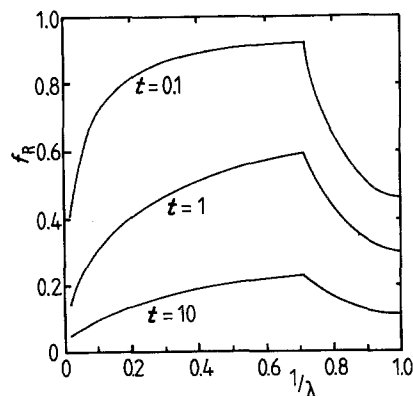


Figure 4 Isochronous Mooney-Rivlin plots of  $f_R$  against  $1/\lambda$  taken from the curves of Fig. 3 for the times shown.

have been plotted in Fig. 7 assuming the values of  $N_0$ ,  $N_p$ ,  $q$  and  $\tau$  as shown in the figure caption and including an additional  $N_p kT$  term in Equation 26 as discussed previously.

In Fig. 8, isochronous data obtained from stress-relaxation curves published by Kusamizu and Ninomiya [10] for relaxation of a styrene-butadiene copolymer (SBR) have been plotted, indicating similar behaviour to that predicted by the model, with  $\lambda_k \sim 1.4$ . (The SBR data have also been published in Ferry [1], p. 427). The predicted curves using Equations 26 and 27 have been plotted on Fig. 8, using the assumed values of the material parameters given in the figure caption.

Further data on the stress relaxation of uncross-linked polymers have been obtained by Ferry and co-workers [11, 12] where, unlike the abovementioned results, the Mooney-Rivlin plot is linear over a range of  $\lambda$  values  $2 \geq \lambda \geq 1.15$ . If, for these two materials,  $\lambda_k$  was less than 1.15, the results would be consistent with the above model, the linear plots being obtained from the region where  $\lambda > \lambda_k$ . (The materials studied were 1,2 polybutadiene [11] and polyisobutylene [12].)

### 4. Discussion

#### 4.1. The knotting elongation, $\lambda_k$

It can be seen that the predictions of the model are

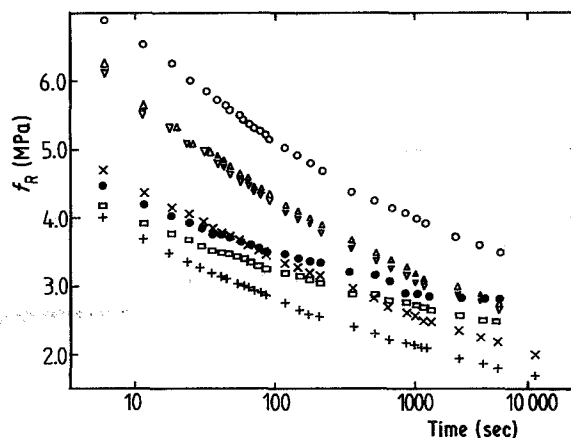


Figure 6 Stress-relaxation curves of reduced stress  $f_R$  against  $\log(t)$  for the various values of  $\lambda$ , for plasticized poly(vinyl chloride) (PPVC) at 21°C.  $\lambda = (\bullet)$  1.10,  $(\square)$  1.14,  $(\circ)$  1.25,  $(\Delta)$  1.37,  $(\nabla)$  1.43,  $(\times)$  1.5,  $(+)$  2.0.

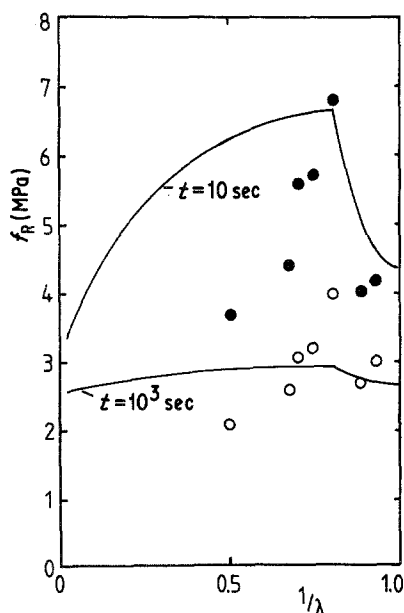


Figure 7 Isochronous Mooney–Rivlin plots taken from the data of Fig. 6 for 10 sec (solid points) and  $10^3$  sec (open circles) compared with the predictions of the model (solid line) with  $N_0kT = 8$  MPa,  $N_1kT = 10$  MPa,  $N_p kT = 2.5$  MPa,  $\tau = 2$ ,  $\lambda_k = 1.25$  and assuming  $q = 1$ .

qualitatively consistent with the experimental results as shown in Figs. 7 and 8, and with the results of Ferry and co-workers [11, 12] if suitable values of  $\lambda_k$  are assumed for each material.

Although little information is available on the styrene–butadiene copolymer, it is likely that it contains some regions of strong molecular interaction due to the styrene portions of the copolymer, and that weaker entanglement interactions occur on the rubbery butadiene segments. A similar heterogeneous arrangement of interactions is also expected in plasticized PVC due to the small amount ( $\sim 5\%$ ) of crystallinity that is thought to exist [13, 14] in this polymer. Such a system of heterogeneous intermolecular interactions is likely to be one in which loose topological knots get tightened by deformation as the strongly

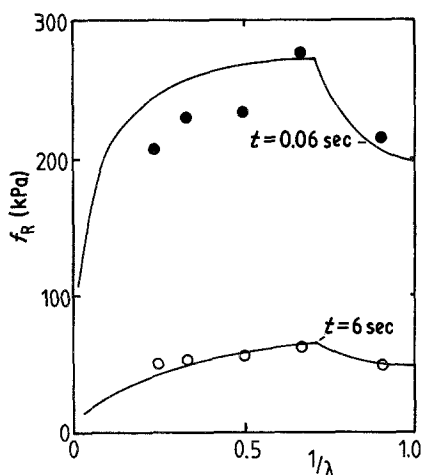


Figure 8 Isochronous Mooney–Rivlin plots taken from stress-relaxation data for a styrene–butadiene copolymer [10] for 0.6 sec (solid points) and 6 sec (open circles) compared with the predictions of the model with  $N_0kT = 220$  kPa,  $N_1kT = 80$  kPa,  $N_p kT = 0$ ,  $\tau = 1$ ,  $\lambda_k = 1.4$  and assuming  $q = 1$ . These data have been reduced to  $80^\circ\text{C}$ .

interacting portions corresponding to F in Fig. 1 (“F-links”) exert forces on the more loosely interacting chain segments. The amount of deformation required to tighten these knots completely will essentially depend inversely on the separation of these F-links, indicating that the SBR has fewer of these than the PPVC.

On the other hand, the two polymers studied by Ferry and co-workers do not display the behaviour interpreted above as the tightening of entanglements. No mention of any crystalline phase is made in the descriptions of the polymers [11, 12], and so it is to be expected that the intermolecular interactions in these polymers are relatively homogeneous. In terms of the model outlined here, the interpretation of the results is that the tightening of the knots occurs at very small elongations as each entanglement is equivalent, and there are none which pull on, and tighten, the neighbouring entanglements.

#### 4.2. Entanglement density $N_E$

The entanglement density  $N_E$  was assumed empirically to increase with deformation as defined by Equation 27. Regarding the three empirical constants in this equation, if we assume that  $q = 1$  then the values of  $N_0kT$  and  $N_1kT$  that roughly fit the experimental data are both of order  $\sim 10$  MPa for the PPVC and less than 1 MPa for the SBR. In the model,  $N_0$  and  $N_1$  are the number of tight entanglements per unit volume at the start of deformation and introduced after an elongation of  $\lambda_k$ , respectively, and the above values correspond satisfactorily with the entangled compliances calculated for a wide variety of polymers (see Ferry [1], p. 406). Such order-of-magnitude agreement is perhaps all that can be expected of such an elementary model.

#### 4.3. The crosslink density $N_p$

In fitting the theoretical curves to the experimental data it was necessary to assume for PPVC that the permanent crosslink density  $N_p$  was non-zero to obtain the rough agreement shown in Fig. 7, whereas the reasonable agreement displayed in Fig. 8 for SBR was obtained by taking  $N_p = 0$ .

This observation could be taken as indicating that PPVC can be considered as a viscoelastic solid in that the stress will not eventually relax to zero, whereas the SBR may perhaps be a viscoelastic fluid in the general sense as defined by Ferry [1].

#### 4.4. The relaxation time

The simple model outlined above is essentially a single relaxation-time model, except that some spread of relaxation times about this single relaxation time is expected due to the anticipated spread in  $n_0$  values ignored in order to simplify the analysis. The deformation-dependent relaxation time is given jointly by Equations 28 and 19 in terms of the model, but the resultant expression is obviously an oversimplification for a number of reasons. Firstly, in any real system some degree of polydispersity is expected, and entanglements would anyway be expected to form at random separations along a polymer chain. One way to allow

for this would be again to allow a spread of relaxation times. Secondly, the restriction defined by Equation 25 does not allow for more than one entanglement on a given polymer chain to be slipped through. If, as seems likely, there are a number of entanglements along a given chain, then the molecule will have to slip through each in turn. When the endmost entanglement has been slipped through, slippage through the next entanglement along the chain will become the dominant relaxation process, and this in general will have a larger value of  $n_0$  and so a larger relaxation time. Following this idea will lead to a sequence of increasing relaxation times depending on the number of entanglements per molecule and their separation. For simplicity, this will not be included here.

#### 4.5. The model

In the simple model outlined above the connection between macroscopic deformation and the deformation of a single chain, as expressed by Equation 4, was made by assuming the individual chain to be "typical". A more realistic approach would be to consider an arrangement of three chains aligned with the principal axes of deformation [15] or a four-chain model [16] with four slipping and tightening entanglements arranged tetrahedrally around a fixed entanglement. The added complexity introduced by either of these approaches is probably not warranted due to the simple nature of other aspects of the model.

A more serious objection could be raised to the use of Gaussian chain statistics to obtain Equation 14, which gives the force on the chain segment FE in Fig. 1. Implicit in this formula are the assumptions that the chain segment FE is large enough, and that the extension of the chain segments is not too large, for random-chain statistics to apply. This latter objection could be met by using Langevin statistics to obtain an equation to replace Equation 14, for cases where the restriction that  $r \ll nl$  does not apply, but again the added complexity that this would introduce is not warranted.

An estimate of the length of the chain segment FE can be made in terms of the model by assuming some order-of-magnitude values for the dimensions of the molecule. Assuming a cylindrical chain segment of  $n$  links each of length  $l$  and cross-sectional radius  $r$ , the number of these per unit volume will be given by

$$N = \frac{\alpha}{\pi r^2 nl} \quad (29)$$

where  $\alpha$  is a constant ( $\alpha \leq 1$ ) expressing the fractional occupied volume in the polymer melt. If we take  $NkT = 1$  MPa, and suppose that  $r = l = 5 \times 10^{-10}$  m, then assuming  $\alpha = 1$  and  $T = 300$  K, we have  $n \sim 11$ . This indicates that in the case of PPVC the

model is only marginally appropriate in that the values of  $NkT$  needed to fit Equation 26 to the data in Fig. 7 are larger than assumed here, and so the predicted value of  $n$  would be small. This makes the lack of agreement between theory and experiment in Fig. 7 more understandable, but the PPVC data still exhibits the characteristic peak (associated here with entanglement tightening) in the Mooney–Rivlin plot. In the case of SBR the above rough calculation indicates in terms of the model that the chains are quite long, and the application of Gaussian statistics is indeed appropriate. The agreement shown in Fig. 8 between theory and experiment is satisfactory, considering the elementary nature of the model and its assumptions.

#### 5. Conclusions

A simple theory of entanglements in polymer melts tightening during deformation, and of stress relaxation due to slippage through such entanglements, has been developed and the predictions of this theory have been compared with experiment.

For polymer melts in which the intermolecular interactions are expected to be heterogeneous, the stress relaxation isochrones display a distinct maximum in a Mooney–Rivlin plot, in agreement with the theory, whereas this maximum is not observed in results for materials which may have homogeneous molecular interactions.

#### References

1. J. D. FERRY, in "Viscoelastic Properties of Polymers", 2nd Edn (Wiley, New York, 1970).
2. W. OPPERMANN and G. REHAGE, *Coll. Poly. Sci.* **259** (1981) 1177.
3. P. G. DE GENNES, *J. Chem. Phys.* **55** (1971) 572.
4. S. F. EDWARDS, *Proc. Phys. Soc.* **91** (1967) 513.
5. E. DONT, *Polym. Bull.* **7** (1982) 417.
6. R. T. DEAM and S. F. EDWARDS, *Phil. Trans. R. Soc.* **A280** (1976) 317.
7. A. J. CHOMPFF and J. A. DUISER, *J. Chem. Phys.* **45** (1966) 1505.
8. M. DOI, *Polym. Prepr.* **22** (1981) 100.
9. L. R. G. TRELOAR, in "The Physics of Rubber Elasticity" (Clarendon Press, Oxford, 1975).
10. S. KUSAMIZU and N. NINOMIYA, *Nippon Gomu-kaishi* **37** (1964) 184.
11. J. W. M. NOORDERMEER and J. D. FERRY, *J. Polym. Sci.* **14** (1976) 509.
12. C. R. TAYLOR, R. GRECO, O. KRAMER and J. D. FERRY, *Trans. Soc. Rheol.* **20** (1976) 141.
13. A. V. TOBOLSKY, D. CARLSON and N. INDICTOR, *J. Appl. Polym. Sci.* **7** (1963) 393.
14. H. R. BROWN, G. M. MUSINDI and Z. H. STACHURSKI, *Polymer* **23** (1982) 1508.
15. H. M. JAMES and E. GUTH, *J. Chem. Phys.* **11** (1943) 455.
16. P. J. FLORY and J. REHNER, *ibid.* **11** (1943) 512.

Received 28 December 1984  
and accepted 31 May 1985